Polar Geosci., **16**, 76–99, 2003

Timing of thermal events in eastern Dronning Maud Land, East Antarctica

Kazuyuki Shiraishi[1], Tomokazu Hokada[1], C.M. Fanning[2], Keiji Misawa[1] and Yoichi Motoyoshi[1]

[1] *National Institute of Polar Research, Kaga 1-chome, Itabashi-ku, Tokyo 173-8515 (shiraishi@nipr.ac.jp)*
[2] *Research School of Earth Sciences, The Australian National University, ACT 0200, Australia*

(Received March 11, 2003; Accepted June 25, 2003)

Abstract: Using cathodoluminescence (CL) images, the zircons analyzed by K. Shiraishi *et al.* (J. Geol., **102**, 47, 1994) for SHRIMP U-Pb dating (prior to the use of CL images) have been re-examined in order to unravel the periods of multiple zircon growth in eastern Dronning Maud Land. In addition four new SHRIMP U-Pb zircon age determinations are presented: two from the Yamato Mountains and two from the Lützow-Holm Complex (LHC). The major conclusion from this study is that the Grenvillian basement is not ubiquitous in the LHC. Some outcrops are of late Archean-Paleoproterozoic crustal fragments reworked during the Pan-African event. In such cases, there is no indication of a Grenvillian event. Other protoliths are derived from Meso-Neoproterozoic juvenile crust and recycled continental sediments from the margin of the craton. Thus the pre-history of the Pan-African LHC is not uniform. In the Yamato Mountains, two stages of the Pan-African event are suggested, at ~620 Ma and ~535 Ma. These two stages are similar to those recorded in the Sør Rondane Mountains and central Dronning Maud Land further to the west. These new and revised, updated results provide important constraints on tectonic models for the formation of Gondwana.

key words: CL image, SHRIMP U-Pb zircon age, Pan-African, East Antarctica, Gondwana

1. Introduction

Pan-African orogenic events in Dronning Maud Land (DML) and other regions of East Antarctica have been widely recognized during the last decade (*e.g.* Shiraishi *et al.,* 1991, 1994; Jacobs *et al.,* 1998; Fitzsimons, 2000; Paech, 2001; Boger *et al.,* 2001; Jacobs, 2002). Precise multi-isotope studies have revealed that there are multiple thermal events during the prolonged history in the region. We have been using SHRIMP U-Pb zircon dating to reveal the timing of each event with respect to the tectonic process and the mutual relationships between the different areas.

Shiraishi *et al.* (1994) presented SHRIMP U-Pb zircon ages for the Lützow-Holm Complex (LHC) and Yamato-Belgica Complex (YBC), and documented for the first time the presence of a Cambrian orogenic belt in East Antarctica (Fig. 1). However,

for the older thermal events, there remain ambiguities as to whether the ~1000 Ma Grenvillian ages are ubiquitous or not. A significant advance since the publication of Shiraishi *et al.* (1994) has been the application of cathodoluminescence (CL) images to clarify and examine the internal structures of zircon (see Rubatto and Gebauer, 2000 for summary). This paper revisits the timing of the thermal events in the Lützow-Holm Complex and the Yamato-Belgica Complex in the light of CL images from the samples used by Shiraishi *et al.* (1994). In addition, we present four new SHRIMP U-Pb zircon age determinations, two from the Yamato Mountains and two from the Lützow-Holm Complex and compare the thermal events between the two complexes.

2. Outline of geology and previous geochronological work

The Lützow-Holm Complex (LHC) is a medium-pressure type metamorphic belt which extends for 300 km along the Prince Olav Coast and Lützow-Holm Bay region in eastern Dronning Maud Land (Fig. 1). The metamorphic grade increases from upper amphibolite-facies in the east to granulite-facies in the southwest (Hiroi *et al.,* 1991). The maximum peak metamorphic conditions for the granulite-facies metamorphism reached *ca.* 1000°C and 11 kbar at Rundvågshetta (Motoyoshi and Ishikawa, 1997). The Yamato-Belgica Complex (YBC) is exposed in the inland mountains to the

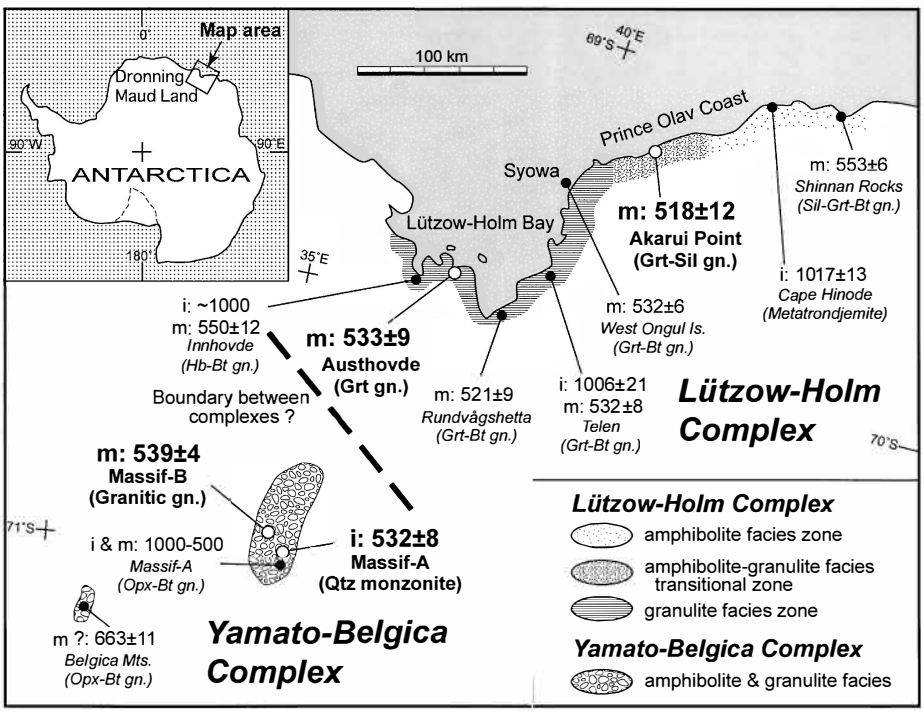

Fig. 1. Map indicating the sample localities. Open symbol shows rocks analyzed in this study. Broken line shows the inferred boundary of the complexes. i: magmatic age, m: metamorphic age.

southwest of the LHC. The complex is characterized by widespread Pan-African granite and syenite intrusions. The metamorphic rocks are mainly composed of amphibolite-facies quartzofeldspathic and intermediate gneisses. Minor amounts of low-pressure granulite-facies rocks occur as large blocks within the syenitic bodies. Contrasting geological and petrological features such as the regional metamorphism pressure type between LHC and YBC have been interpreted as resulting from a continent-continent collision (*e.g.* Hiroi *et al*., 1991). In the last two decades, radiometric ages using high closure temperature isotopic systems such as Rb-Sr and Sm-Nd whole-rock systems have been reported from both complexes, but no conclusive geochronologic interpretation was obtained for the high grade event (*e.g.* Shibata *et al.,* 1986; Nishi *et al.,* 2002 and references herein). Shiraishi *et al.* (1994) reported SHRIMP U-Pb zircon ages for eight rocks from this area; these data placed the first time constraints on the early Paleozoic peak metamorphic event. However, these SHRIMP data are limited and there remain some ambiguities on older events because the internal structure of the zircon grains was not clear. Subsequently Fraser (1997) reported SHRIMP zircon ages of the seven rocks from the LHC and confirmed that orogenesis took place in Pan-African times. Fraser (1997) also proposed that high-grade metamorphic conditions prevailed for at least 40 Ma (~560–520 Ma) and perhaps as long as 100 Ma (~620–520 Ma). Asami *et al.* (1997) suggested that high-grade Cambrian (530–550 Ma) metamorphism is widespread in East Antarctica from CHIME dating of monazites from some metamorphic rocks from an extensive area of eastern Dronning Maud Land.

3. CL imaging for previously analyzed zircons

In order to clarify the internal structure of zircons, the cathodoluminescence (CL) images were taken from samples used for the previously published SHRIMP study (Shiraishi *et al.,* 1994). Most of these samples are of metasedimentary rocks (paragneisses) with a few meta-igneous rocks (orthogneisses and meta-volcanics), as deduced from geological, petrological and chemical constraints. To avoid duplication of descriptions, only the characteristic features revealed by the CL images are described here. For the nomenclature and interpretation of the zonal structure of zircon grains, we referred to Vavra *et al.* (1996, 1999) and Rubatto and Gebauer (2000). The CL images were obtained using a JEOL scanning electron microscope (JSM-5900LV) with an Oxford Mono-CL at the National Institute of Polar Research (NIPR). The spot numbers shown in Figs. 2–6 are the same as those given in Shiraishi *et al.* (1994). Because some samples were lost, and also due to space limitation, not all CL images for this study are shown.

3.1. Sample 73123106: Metatrondjemite, Cape Hinode (Fig. 2)

Most zircons are elongate with subround terminations. The CL images reveal a dominant simple oscillatory zonation with only very thin homogeneous rims and embayments observed on some grains. The oscillatory zoned areas are clearly of a magmatic nature, whilst the thin rims and embayed areas are interpreted to be metamorphic in origin (*e.g.* Rubatto and Gebauer, 2000). From these images, it is now evident

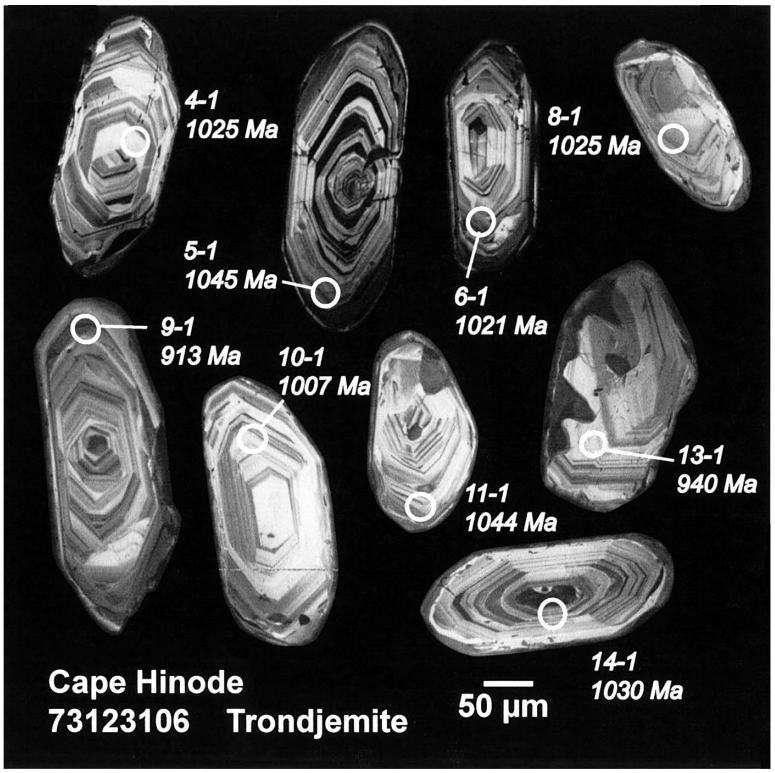

Fig. 2. Cathodoluminescence images of zircons analyzed with ion-microprobe (Sp. 73123106: Cape Hinode). Spot locations and numbering and SHRIMP ages ($^{206}Pb/^{238}U$ ages).

that all the spots analyzed are on the inner magmatic core and so relate to the crystallization age of the igneous protolith. Overgrowth formation during metamorphism would be restricted because of the very limited supply of zirconium bearing fluid. This interpretation is supported by the small amounts of hydro-silicates such as biotite and hornblende in this rock. Grain 13 is largely resorbed by the later event, possibly during the peak metamorphism (Pan-African age).

Crystallization of trondhjemitic magma at ~1000 Ma is consistent with the whole-rock isochron ages of Sm-Nd and Rb-Sr systems (Shiraishi *et al*., 1995).

3.2. Sample 81012803: Garnet-biotite gneiss, West Ongul Island (Fig. 3)

A variety of zircon morphologies are present in this sample. Under CL, there are both round and faceted (pyramidal) homogeneous rims to grains interpreted to have cystallized during the peak metamorphic event (510–550 Ma). The internal parts of some grains also have a variety of zoned and homogeneous CL structures, recording a wide range of Paleo-Mesoproterozoic inherited ages. It is also possible that the core of some grains, for example, the magmatically zoned core of grains 7 and 18, show the effects of transport prior to metamorphism, suggesting a detrital origin for such cores. Analysis 6-1 records a $^{207}Pb/^{206}Pb$ age of ~2740 Ma, the oldest inherited age in this rock.

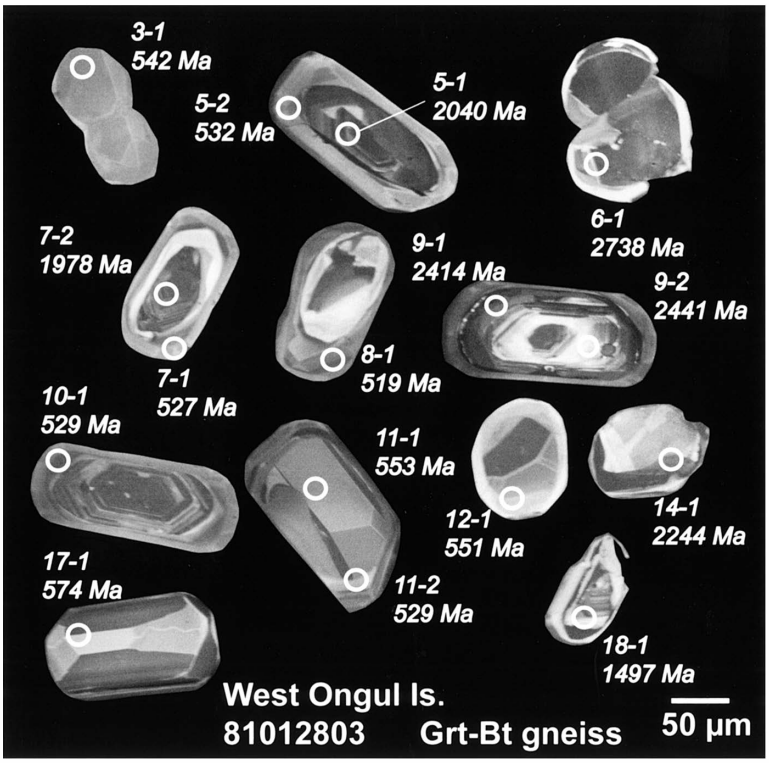

Fig. 3. Cathodoluminescence images of zircons analyzed with ion-microprobe (Sp. 81012803: West Ongul Island). Spot locations and numbering and SHRIMP ages ($^{206}Pb/^{238}U$ ages and the older ages than ~1500 Ma are given as $^{207}Pb/^{206}Pb$ ages) are indicated.

There is no record for zircon growth at ~1000 Ma, although a light narrow layer surrounded by ~525 Ma rim in grain 7 and partial resorption of the inherited core in grain 8 (8-1) may reflect other ages for zircon growth.

3.3. Sample 20112A: Garnet-biotite gneiss, Telen (Fig. 4)

This is the only pelitic rock sample in LHC that records both ~1000 Ma and much older (>1500 Ma) inherited zircon cores overgrown or resorbed by the later Pan-African events. Analyses 9-1, 11-1 and 12-1 appear as optically simple areas within the respective grains, however, the location on the CL image reveals that these analyses are of mixed areas, while others are measured on single domains. In general, the ~1000 Ma inherited cores have igneous zonation with high Th/U ratios (>0.25) (Rubatto and Gebauer, 2000). Thus this metasedimentary rock is interpreted to have a Grenville age magmatic zircon detritus. There is no record of ~1000 Ma overgrowths surrounding older Meso-Paleoproterozoic inherited cores. The protolith would be a mixture of Meso-Paleoproterozoic continental crust and Grenvillian magmatic source.

3.4. Sample RH-112-20B: Garnet-biotite gneiss, Rundvågshetta (Fig. 5a)

The zircons analyzed from this sample are dominantly round to elongate grains.

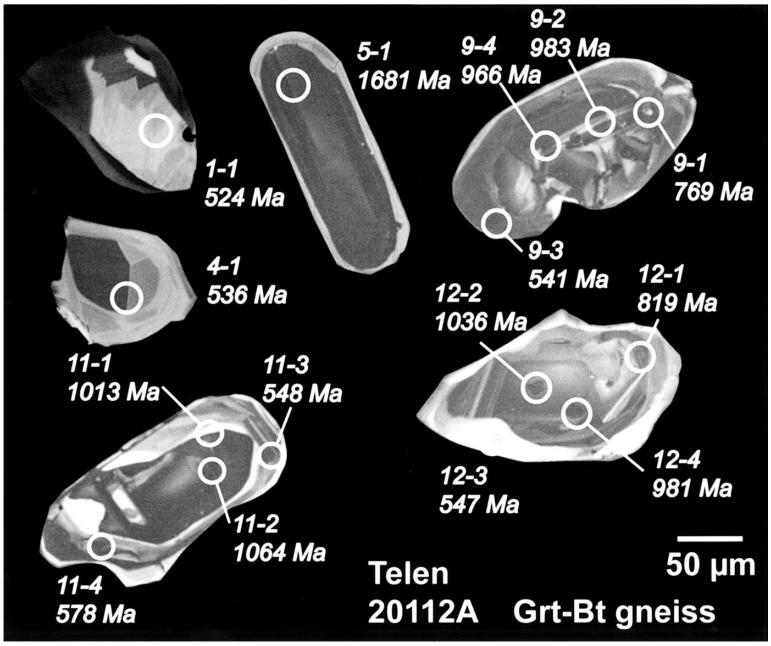

Fig. 4. Cathodoluminescence images of zircons analyzed with ion-microprobe (Sp. 20112A: Telen). Spot locations and numbering and SHRIMP ages ($^{206}Pb/^{238}U$ ages and the older ages than ~800 Ma are given as $^{207}Pb/^{206}Pb$ ages) are indicated.

Many of the grains have inherited cores recording late Archean to Paleoproterozoic ages. Others appear to be recrystallized, homogeneous grains with surfaces rounded by resorption. The location of analysis 22-1 shows this analysis to be of a mixed area. The core part of grain 22 with fragmental zoning structure suggests a detrital origin as well as the other cores showing $>$2500 Ma. Notwithstanding that no age determination was performed for a narrow dark zone between spot 3-1 (2505 Ma) and 3-2 (569 Ma), from the current data there is no indication of ~1000 Ma age in this rock. Fraser (1997) also performed SHRIMP zircon age determination for various rock types from Rundvågshetta, and no ~1000 Ma zircon growth was obtained.

3.5. Sample 8401106: Hornblende-biotite gneiss, Innhovde (Fig. 5b)

This rock is thought to be meta-igneous in origin (Shiraishi *et al*., 1994). Elongated grains with round to subround terminations are consistent with formation during high-grade metamorphism. Analyses 4-1 and 6-1 record $^{206}Pb/^{238}U$ ages of ~1000 Ma, suggesting that the age of crystallization of the igneous core to these grains is Grenville. Spot 3-1 seems to be affected by younger metamorphic resorption. With the additional evidence of the CL images, this rock is interpreted to be a ~1000 Ma igneous rock of intermediate composition that was metamorphosed during the Pan-African event.

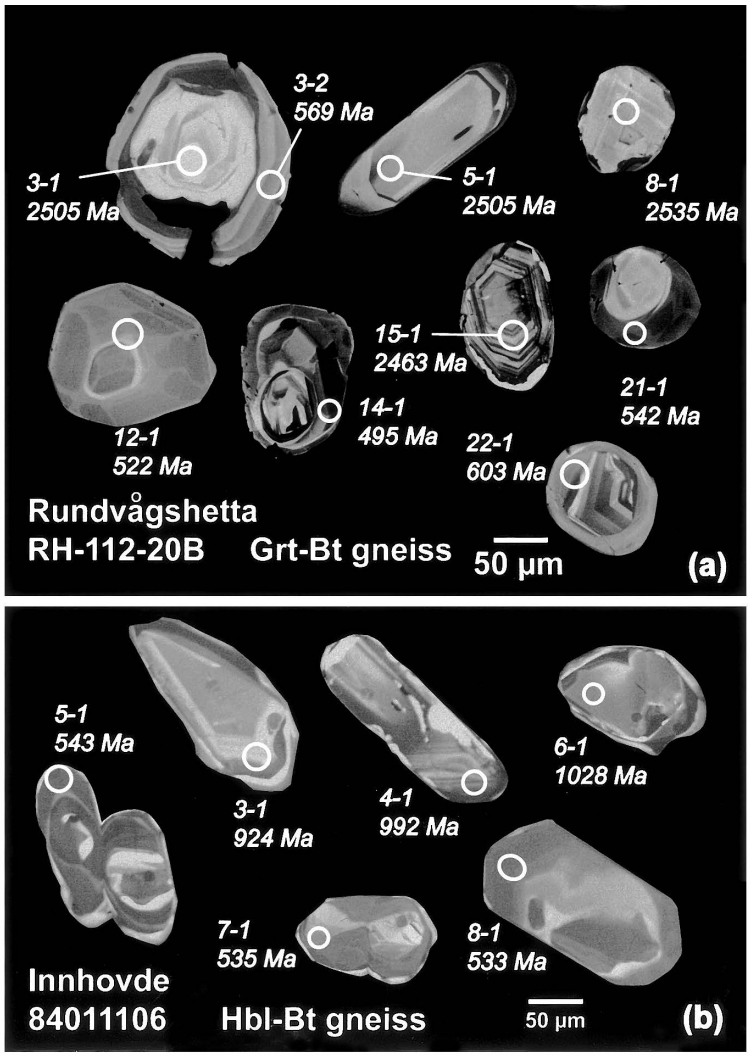

Fig. 5. Cathodoluminescence images of zircons analyzed with ion- microprobe. Spot locations and numbering and SHRIMP ages ($^{206}Pb/^{238}U$ ages) are indicated. a: Sp. RH112-20B (Rundvågshetta). b. Sp. 84011106 (Innhovde).

3.6. Sample Y80A530: Orthopyroxene biotite gneiss, the southern Yamato Mountains (Fig. 6a)

Most grains have complexly structured cores surrounded by metamorphic overgrowths. SHRIMP analyses for nineteen areas do not define unique age groupings (Shiraishi *et al.*, 1994, Fig. 9). The ~750 Ma ages such as spots 3-1 (not shown), 7-1 and 8-1 are seen from the CL images to be mixed ages. Analysis 1-1 is of the low luminescent rim to a grain that has a core showing fir-tree sector zoning. Spot 13-1 that is discordant with a $^{207}Pb/^{206}Pb$ age of ~2470 Ma records the oldest age analyzed in the sample although an older inherited core is visible in this grain. Spot 14-1 yields an

intermediate $^{206}Pb/^{238}U$ age of ~774 Ma from the low luminescent margin of the central component of this grain, and is surrounded by another low luminescent external rim. It is not certain whether this intermediate age is the result of resorption of the inherited core or the age of new overgrowth. The secondary high U overgrowths were obtained only from three rims of spots 2-2 (613 Ma), 8-2 (605 Ma) and 16-1 (633 Ma) (not shown).

3.7. Sample A79121511: Biotite gneiss, Belgica Mountains (Fig. 6b)

The CL images confirm that spots 7-1 (not shown) and 13-1 are mixed ages. Spots 5-1 (not shown) and 6-1 show radiogenic Pb loss on the Tera and Wasserburg diagram

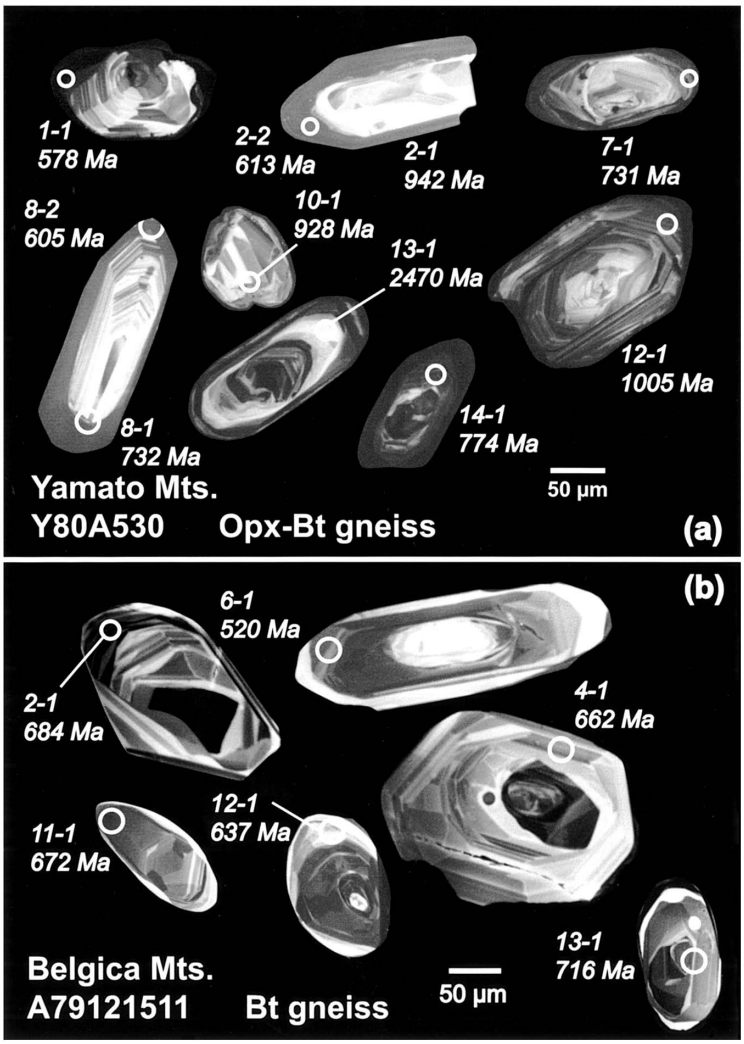

Fig. 6. Cathodoluminescence images of zircons analyzed with ion-microprobe. Spot locations and numbering and SHRIMP ages ($^{206}Pb/^{238}U$ ages) are indicated. a: Sp. Y80A530 (Massif A, Yamato Mountains). Note: Only spot 13-1 is shown by a $^{207}Pb/^{206}Pb$ age. b: Sp. A79121511 (Belgica Mountains).

and the areas analyzed are from the resorbed areas near the grain margins. Many other marginal areas analyzed record discordant ~660 Ma ages. However, there are external thin rims ($<10\,\mu$m in width) that may record a younger metamorphic age.

4. SHRIMP analyses

We obtained new SHRIMP U-Pb zircon ages for two rocks each from LHC and from the southern part of the Yamato Mountains, respectively (Fig. 1).

4.1. Analytical procedures

Zircons from LHC and YBC were analyzed for U, Th and Pb using the SHRIMP II ion microprobe at ANU in Canberra and at NIPR in Tokyo. Instrumental conditions and measurement procedures at both institutes were the same, and similar to those described in Williams (1998). The CL information was obtained prior to the SHRIMP analyses for the new samples using a HITACHI S-2250N SEM fitted with an internal parabolic mirror to boost signal strength at ANU and a JEOL scanning electron microscope (JSM-5900LV) with an Oxford Mono-CL at NIPR. A ~30 μm diameter analytical spot was used for the SHRIMP analyses, and secondary ions were measured at a mass resolution of ~5500. U concentrations are relative to the Sri Lankan zircon SL13 (U = 238 ppm; $^{206}Pb/^{238}U$ age of 572 Ma; Compston, 1999). Pb/U ratios were corrected for instrumental mass fractionation using ratios measured on the FC1 reference zircon (1099 Ma; Paces and Miller, 1993). Data reduction and processing were conducted using the computer programs SQUID ver. 1 and ISOPLOT ver. 2 provided by K.R. Ludwig at the Berkeley Geochronology Center (Ludwig, 2001a, b). The errors of each analysis shown in Tables 1–4 are at 1-sigma (*c.* 68% confidence level).

4.2. Sample 92012302: Garnet-sillimanite gneiss, Akarui Point

Akarui Point is situated in the transitional zone between amphibolite and granulite facies zones in LHC (Fig. 1). The sample is a garnet-sillimanite-gneiss of pelitic composition. There are abundant zircons that have round to sub-round outlines and essentially simple clear interiors. Only three CL images of this sample are available because the specimen has been lost. Under the microscope, the zircon population is dominated by simple clear round grains that are thought to have formed during high grade metamorphism. However, CL images revealed that some grains (5, 6, 7) have cores surrounded by outer rims (Fig. 7a).

Twenty analyses were performed on 15 grains. Many grains were analyzed near the center, or on areas representing inherited zircon components. On a Tera and Wasserburg concordia plot there is a dominant cluster of analyses on or near concordia at about 520 Ma (Fig. 8). Three of the central areas analyzed yield significantly older ages (analyses 4-1, 13-1 and 14-1) ranging up to about 840 Ma. No Meso-Paleoproterozoic inheritance was determined in the 15 grains analyzed, even though centers and other possible anomalous areas were targetted. BEI images show that fine cracks run through the spot 5-1 and the age obtained is not accurate. Grains 6 and 7 are crystallized during the Pan-African and younger overgrowth is evident (spot 7-2).

Table 1. Summary of ion microprobe U-Pb results for zircons from Sp. 92012302.

Grain spot	U (ppm)	Th (ppm)	Th/U	$^{206}Pb^*$ (ppm)	$^{204}Pb/^{206}Pb$	f206 (%)	Total Ratios $^{238}U/^{206}Pb$	±	$^{207}Pb/^{206}Pb$	±	Radiogenic $^{206}Pb/^{238}U$	±	Age (Ma) $^{206}Pb/^{238}U$	±
1.1	754	11	0.01	56.3	0.000020	<0.01	11.499	0.129	0.0580	0.0006	0.0870	0.0010	537.7	5.9
1.2	190	6	0.03	14.2	0.000253	0.14	11.516	0.208	0.0593	0.0011	0.0867	0.0016	536.1	9.5
2.1	265	8	0.03	19.3	0.000070	0.26	11.811	0.152	0.0599	0.0010	0.0845	0.0011	522.6	6.6
3.1	187	7	0.04	13.7	0.000146	0.52	11.759	0.163	0.0621	0.0012	0.0846	0.0012	523.5	7.1
3.2	145	2	0.01	10.2	0.000073	0.33	12.125	0.181	0.0601	0.0014	0.0822	0.0013	509.2	7.5
4.1	577	207	0.36	55.3	0.000095	0.58	8.953	0.104	0.0669	0.0006	0.1111	0.0013	678.9	7.7
4.2	457	10	0.02	35.1	0.000212	0.42	11.191	0.136	0.0620	0.0007	0.0890	0.0011	549.5	6.5
5.1	469	14	0.03	33.2	0.000280	0.43	12.160	0.141	0.0609	0.0009	0.0819	0.0010	507.4	5.8
6.1	146	13	0.09	10.6	-	0.32	11.794	0.176	0.0604	0.0014	0.0845	0.0013	523.0	7.7
7.1	1232	15	0.01	92.5	0.000009	0.06	11.443	0.123	0.0587	0.0004	0.0873	0.0010	539.8	5.7
7.2	220	21	0.09	16.0	0.000263	0.28	11.807	0.155	0.0601	0.0010	0.0845	0.0011	522.7	6.8
8.1	227	3	0.01	16.4	0.000196	0.42	11.925	0.160	0.0611	0.0010	0.0835	0.0011	517.0	6.8
9.1	340	16	0.05	26.8	0.000028	0.32	10.899	0.133	0.0615	0.0012	0.0915	0.0011	564.1	6.7
10.1	1276	31	0.02	88.9	0.001294	2.56	12.331	0.131	0.0778	0.0011	0.0790	0.0009	490.3	5.4
11.1	335	11	0.03	23.7	0.000130	0.26	12.128	0.151	0.0596	0.0008	0.0822	0.0010	509.5	6.2
12.1	269	8	0.03	19.5	0.000022	0.12	11.818	0.151	0.0588	0.0009	0.0845	0.0011	523.0	6.6
13.1	541	203	0.37	65.2	0.000000	0.22	7.133	0.088	0.0690	0.0012	0.1399	0.0018	844.0	10.1
13.2	974	14	0.01	70.2	0.000019	0.09	11.913	0.128	0.0585	0.0004	0.0839	0.0009	519.1	5.5
14.1	718	141	0.20	69.5	0.000009	0.43	8.869	0.096	0.0659	0.0005	0.1123	0.0012	685.9	7.2
15.1	1131	15	0.01	82.7	0.000095	0.11	11.747	0.125	0.0588	0.0004	0.0850	0.0009	526.1	5.5

Notes:

1. Uncertainties given at the one sigma level.
2. Error in SL13 reference zircon calibration was 1.72% & 1.27% respectively for the two analytical sessions (not included in above errors but required when comparing data from different mounts).
3. f206% denotes the percentage of ^{206}Pb that is common Pb.
4. Correction for common Pb made using the measured $^{238}U/^{206}Pb$ and $^{207}Pb/^{206}Pb$ ratios following Tera and Wasserburg (1972) as outlined in Williams (1998).

Table 2. Summary of ion microprobe U-Pb results for zircons from Sp. 93012401A.

Notes: 1. Uncertainties given at the one sigma level.
2. Error in SL13 reference zircon calibration was 0.62% for the analytical sessions (not included in above errors but required when comparing data from different mounts).
3. f206% denotes the percentage of ^{206}Pb that is common Pb.
4. For analyses >800 Ma correction for common Pb made using the measured ^{204}Pb/^{206}Pb ratio.
5. For analyses <800 Ma correction for common Pb made using the measured ^{238}U/^{206}Pb and ^{207}Pb/^{206}Pb ratios following Tera and Wasserburg (1972) as outlined in Williams (1998).
6. For % Disc, 0% denotes a concordant analysis.

Table 3. Summary of ion microprobe U-Pb results for zircons from Sp. Y80A544.

Grain spot	U (ppm)	Th (ppm)	Th/U	$^{206}Pb^*$ (ppm)	$^{204}Pb/^{206}Pb$	f206 (%)	Total Ratios $^{238}U/^{206}Pb$	±	$^{207}Pb/^{206}Pb$	±	Radiogenic $^{206}Pb/^{238}U$	±	Age (Ma) $^{206}Pb/^{238}U$	±
1.1	97	119	1.23	7.2	0.000454	0.46	11.691	0.172	0.0616	0.0016	0.0851	0.0013	526.8	7.7
2.1	222	105	0.47	17.6	0.003204	5.11	10.817	0.141	0.1000	0.0031	0.0877	0.0014	542.0	8.0
2.2	278	131	0.47	19.9	0.000166	0.48	12.032	0.226	0.0614	0.0007	0.0827	0.0016	512.3	9.4
3.1	260	171	0.66	19.3	0.000049	<0.01	11.569	0.158	0.0577	0.0007	0.0865	0.0012	534.7	7.2
3.2	265	192	0.73	19.8	-	0.17	11.463	0.163	0.0596	0.0007	0.0871	0.0013	538.3	7.5
4.1	249	215	0.86	19.1	-	0.10	11.208	0.145	0.0594	0.0008	0.0891	0.0012	550.4	7.0
4.2	400	187	0.47	30.3	0.000043	<0.01	11.363	0.157	0.0580	0.0006	0.0880	0.0012	544.0	7.3
4.3	226	192	0.85	16.3	0.000290	0.41	11.892	0.147	0.0610	0.0007	0.0837	0.0011	518.5	6.3
5.1	323	115	0.36	24.0	0.000150	0.03	11.555	0.145	0.0584	0.0006	0.0865	0.0011	534.9	6.6
6.1	249	212	0.85	19.6	0.000009	<0.01	10.934	0.145	0.0584	0.0007	0.0915	0.0012	564.5	7.3
6.2	311	136	0.44	23.0	0.000012	0.11	11.624	0.226	0.0589	0.0007	0.0859	0.0017	531.5	10.1
6.3	294	238	0.81	21.4	-	0.14	11.784	0.141	0.0590	0.0006	0.0847	0.0010	524.4	6.1
7.1	683	109	0.16	67.3	0.000128	0.14	8.717	0.102	0.0639	0.0004	0.1146	0.0014	699.2	8.0
8.1	391	204	0.52	29.4	0.000034	0.08	11.419	0.141	0.0589	0.0006	0.0875	0.0011	540.8	6.5
8.2	263	321	1.22	19.1	0.000118	0.06	11.820	0.176	0.0583	0.0007	0.0846	0.0013	523.2	7.6
9.1	1439	75	0.05	112.7	0.000005	0.06	10.973	0.138	0.0594	0.0004	0.0911	0.0012	561.9	6.9
9.2	1415	89	0.06	113.2	0.000025	0.14	10.743	0.147	0.0603	0.0005	0.0930	0.0013	573.0	7.6
10.1	280	157	0.56	21.3	0.000065	0.06	11.309	0.144	0.0590	0.0008	0.0884	0.0012	545.9	6.8
11.1	301	144	0.48	22.2	-	0.27	11.665	0.156	0.0602	0.0010	0.0855	0.0012	528.8	7.0
11.2	76	70	0.92	5.6	0.000060	0.18	11.787	0.259	0.0593	0.0013	0.0847	0.0019	524.0	11.3
12.1	259	93	0.36	19.5	0.000145	0.87	11.383	0.145	0.0653	0.0009	0.0871	0.0011	538.3	6.7
13.1	205	121	0.59	15.4	-	<0.01	11.433	0.156	0.0576	0.0010	0.0875	0.0012	540.9	7.2
13.2	90	78	0.87	6.5	-	0.11	11.774	0.189	0.0587	0.0012	0.0848	0.0014	524.9	8.3
14.1	2637	1837	0.70	210.1	0.000075	0.09	10.780	0.144	0.0599	0.0002	0.0927	0.0013	571.3	7.4
15.1	9949	965	0.10	873.9	0.000006	<0.01	9.781	0.125	0.0603	0.0001	0.1023	0.0013	627.8	7.8
16.1	217	239	1.10	15.8	0.000024	0.09	11.795	0.210	0.0586	0.0007	0.0847	0.0015	524.1	9.1
17.1	99	104	1.05	7.0	0.000382	1.03	12.206	0.348	0.0657	0.0015	0.0811	0.0024	502.6	14.0

Notes: 1. Uncertainties given at the one sigma level.
2. Error in FC1 reference zircon calibration was 0.41% for the analytical sessions (not included in above errors but required when comparing data from different mounts).
3. f206% denotes the percentage of ^{206}Pb that is common Pb.
4. Correction for common Pb made using the measured $^{238}U/^{206}Pb$ and $^{207}Pb/^{206}Pb$ ratios following Tera and Wasserburg (1972) as outlined in Compston *et al.* (1992).

Table 4. Summary of ion microprobe U-Pb results for zircons from Sp. Y80B501.

Grain spot	U (ppm)	Th (ppm)	Th/U	$^{206}Pb^*$ (ppm)	$^{204}Pb/^{206}Pb$	f206 (%)	Total Ratios $^{238}U/^{206}Pb$	±	$^{207}Pb/^{206}Pb$	±	Radiogenic $^{206}Pb/^{238}U$	±	Age (Ma) $^{206}Pb/^{238}U$	±
1.1	295	70	0.24	22.9	-	0.15	11.059	0.195	0.0600	0.0010	0.0903	0.0016	557.2	9.6
1.2	206	51	0.25	15.5	-	<0.01	11.455	0.186	0.0577	0.0009	0.0874	0.0014	539.9	8.6
2.1	134	76	0.57	10.9	0.000356	0.15	10.601	0.165	0.0606	0.0010	0.0942	0.0015	580.2	8.8
2.2	313	106	0.34	24.5	-	<0.01	10.956	0.157	0.0582	0.0007	0.0913	0.0013	563.5	7.9
2.3	94	41	0.43	7.2	-	2.11	11.174	0.252	0.0755	0.0015	0.0876	0.0020	541.4	12.0
2.4	130	66	0.51	9.9	0.000103	<0.01	11.295	0.170	0.0574	0.0010	0.0887	0.0014	547.6	8.1
3.2	606	235	0.39	42.2	0.000019	0.20	12.340	0.146	0.0588	0.0008	0.0809	0.0010	501.4	5.8
3.3	807	261	0.32	60.6	0.000079	<0.01	11.448	0.183	0.0577	0.0004	0.0874	0.0014	540.2	8.4
4.1	751	384	0.51	59.3	-	<0.01	10.882	0.128	0.0580	0.0004	0.0920	0.0011	567.4	6.5
4.2	612	228	0.37	43.8	-	0.41	12,010	0.146	0.0609	0.0035	0.0829	0.0011	513.6	6.5
5.1	543	211	0.39	41.3	0.000056	0.09	11.297	0.135	0.0592	0.0005	0.0884	0.0011	546.3	6.4
6.1	529	191	0.36	41.1	0.000013	0.09	11.050	0.135	0.0595	0.0005	0.0904	0.0011	558.0	6.6
8.1	222	162	0.73	19.9	0.000058	0.03	9.567	0.173	0.0613	0.0005	0.1045	0.0019	640.7	11.3
8.2	193	70	0.36	15.2	0.000097	0.19	10.926	0.130	0.0604	0.0014	0.0913	0.0011	563.5	6.6
8.3	198	159	0.80	16.5	-	0.03	10.332	0.150	0.0600	0.0007	0.0968	0.0014	595.4	8.4
9.1	472	31	0.07	42.0	-	0.59	9.653	0.190	0.0657	0.0009	0.1030	0.0021	631.8	12.1
9.2	267	82	0.31	20.0	-	0.23	11.471	0.146	0.0601	0.0009	0.0870	0.0011	537.6	6.7
9.3	737	60	0.08	62.7	0.000001	0.02	10.104	0.118	0.0603	0.0004	0.0990	0.0012	608.3	6.9
10.1	535	176	0.33	40.3	-	<0.01	11.402	0.157	0.0574	0.0005	0.0878	0.0012	542.5	7.3
10.2	499	152	0.31	36.7	-	0.02	11.684	0.221	0.0582	0.0005	0.0856	0.0016	529.3	9.8
11.1	1080	481	0.45	80.0	0.000014	<0.01	11.599	0.180	0.0579	0.0003	0.0862	0.0014	533.2	8.1
12.1	437	133	0.30	32.4	-	<0.01	11.571	0.133	0.0580	0.0004	0.0864	0.0010	534.4	6.0
12.2	498	76	0.15	37.4	0.000065	<0.01	11.435	0.133	0.0561	0.0006	0.0877	0.0010	541.9	6.2
13.1	469	153	0.33	34.0	-	0.06	11.852	0.156	0.0583	0.0004	0.0843	0.0011	521.9	6.7
14.1	298	284	0.95	24.7	-	<0.01	10.358	0.125	0.0595	0.0006	0.0966	0.0012	594.3	7.0
14.2	286	246	0.86	23.4	-	<0.01	10.512	0.207	0.0588	0.0006	0.0952	0.0019	586.3	11.2
15.1	284	139	0.49	22.6	0.000030	0.09	10.784	0.134	0.0598	0.0007	0.0927	0.0012	571.2	6.9
16.1	504	178	0.35	38.7	-	0.06	11.186	0.142	0.0591	0.0005	0.0893	0.0012	551.6	6.9
16.2	377	112	0.30	28.1	0.000082	<0.01	11.508	0.138	0.0581	0.0006	0.0869	0.0011	537.2	6.3
17.1	106	52	0.49	9.4	0.000108	0.26	9.719	0.181	0.0628	0.0011	0.1026	0.0020	629.8	11.4
18.1	757	216	0.29	54.7	0.000012	0.02	11.882	0.180	0.0579	0.0004	0.0841	0.0013	520.8	7.7
19.1	652	234	0.36	46.9	0.000065	0.03	11.939	0.184	0.0580	0.0004	0.0837	0.0013	518.4	7.8
20.1	663	241	0.36	50.2	0.000022	0.09	11 .351	0.125	0.0591	0.0004	0.0880	0.0010	543.8	5.9
21.1	634	284	0.45	46.1	0.000047	0.10	11,797	0.208	0.0586	0.0004	0.0847	0,0015	524.0	9.0
22.1	719	315	0.44	52.9	0.000023	<0.01	11.684	0.135	0.0579	0.0006	0.0856	0.0010	529.5	6.0
23.1	725	247	0.34	51.9	0.000194	0.41	12.009	0.182	0.0609	0.0006	0.0829	0.0013	513.6	7.6
24.1	793	409	0.52	59.2	-	0.01	11.518	0.125	0.0583	0.0004	0.0868	0.0010	536.6	5.7
25.1	660	305	0.46	50.2	-	0.03	11.303	0.125	0.0587	0.0004	0.0884	0.0010	546.3	5.9

Notes: 1. Uncertainties given at the one sigma level.
2. Error in FC1 reference zircon calibration was 0.41% for the analytical sessions (not included in above errors but required when comparing data from different mounts).
3. f206% denotes the percentage of ^{206}Pb that is common Pb.
4. Correction for common Pb made using the measured $^{238}U/^{206}Pb$ and $^{207}Pb/^{206}Pb$ ratios following Tera and Wasserburg (1972) as outlined in Compston *et al*. (1992).

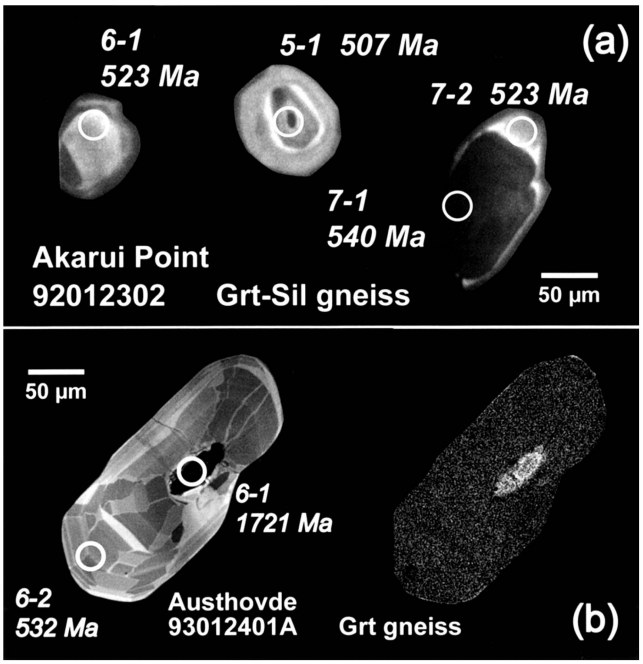

Fig. 7. Cathodoluminescence images of zircons analyzed with ion-microprobe. a: Sp. 92012302 (Akarui Point). Spot locations and numbering and SHRIMP ages ($^{206}Pb/^{238}U$ ages) are indicated. b: Sp. 93012401A (Austhovde). BEI (right) image is also shown. Note the sectored zonal structure (fir-tree structure). SHRIMP $^{206}Pb/^{238}U$ age for rim and $^{206}Pb/^{207}Pb$ age for core are given.

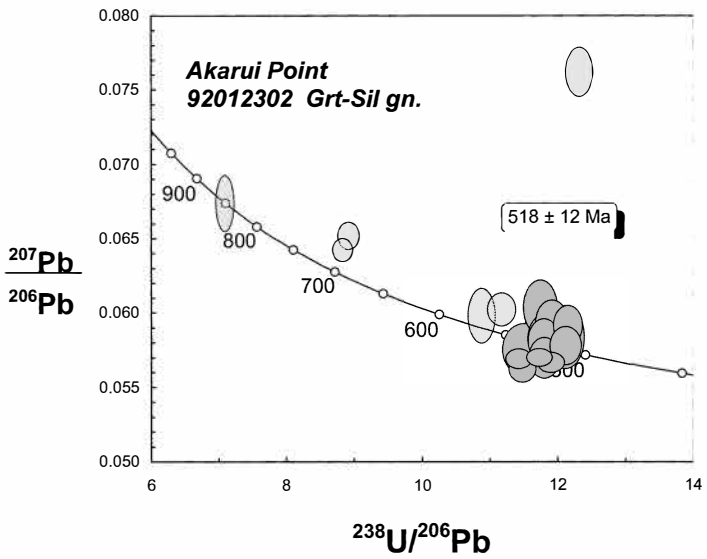

Fig. 8. Tera and Wasserburg (1972) concordia plot of uncorrected U-Pb zircon analyses for Sp. 92012302 (Akarui Point). Analyses plotted with one sigma error bars. Weighted mean of $^{206}Pb/^{238}U$ ages (^{207}Pb corrected, ±95% confidence limits) is shown for the dominant grouping of near, to concordant analyses (darker shaded spots).

Analysis 10-1 is significantly enriched in common lead, and has a $^{206}Pb/^{238}U$ age younger than all the others. Two other analyses yield slightly older $^{206}Pb/^{238}U$ ages than the dominant grouping; Spot 4-2 at about 550 Ma and 9-1 at about 560 Ma. A weighted mean of the $^{206}Pb/^{238}U$ ratios for the remaining 9 analyses for the clear rounded grains has no excess scatter at 518±12 Ma. This gives the crystallization age of the dominat zircon component which is considered to have formed during high grade metamorphism.

4.3. Sample 93012401A: Garnet-sillimanite gneiss, Austhovde

This sample is a pelitic gneiss, consisting of garnet, sillimanite, perthite, plagioclase, quartz with minor biotite, ilmenite, hercynite, rutile and zircon. A large number of optically clear, structureless zircons were separated from this sample. The zircons are relatively large and round to sub-round in outline. For the same reason as for the sample from Akarui Point, only one CL image was obtained. The CL image reveals fir-tree sector zoning, typically observed in the overgrowth of granulite zircons, suggesting a rapid fluctuating growth rate (Vavra *et al.,* 1996) (Fig. 7b). Part of the rim is resorbed by the later event.

Only 13 analyses have been completed on 7 grains (Fig. 9). Centers and rims of 6 of the grains have been analyzed; the centers are either grouped with the rims at about 540 Ma or reflect older ages. Analyses of the centers of grains 4 (4-1), 6 (6-1) and 7 (7-1) yield discordant results with $^{207}Pb/^{206}Pb$ ages of 3450, 1721 and 2078 Ma respectively (^{207}Pb corrected). Analysis 4-1 is significantly enriched in common Pb and gives no meaningful age. An analysis near the center of grain 5 (5-2) is reversely discordant and there is no obvious reason for this anomalous analysis. The U and Th contents are similar to others from this sample, the area analyzed appears to be clear and simple. The core analysis of grain 2 (2-1) is also anomalous. The remaining 8 analyses cluster on or near concordia. An analysis, 3-1, shows slightly older age than the seven other analyses. A weighted mean of the ^{207}Pb corrected $^{206}Pb/^{238}U$ ages has no excess scatter at 533±9 Ma. From the present data, it is concluded that 533 Ma represents the time of dominant zircon growth during high grade metamorphism and the inherited Protoproterozoic cores are detrital in origin.

Fraser (1997) reported SHRIMP zircon ages from a gneissic granite from Austhovde and concluded that the rock experienced two stages of Pan-African zircon growth, at ~549 Ma and 506 Ma. However our data do not permit distinguishing two stages of metamorphism.

4.4. Sample Y80A544: Quartz monzonite, Massif-A of the Yamato Mountains

This rock is a quartz monzonite from the northern end of Massif-A of the Yamato Mountains. The rock is a light grey to brown-coloured, homogeneous, medium- to coarse-grained rock consisting of clinopyroxene, biotite, K-feldspar, plagioclase and quartz, with or without dark green hornblende. Accessory minerals are titanite, apatite, zircon, ilmenite, pyrite, allanite, and pyrrhotite. The rock intrudes into the quartz syenitic charnockite with diffuse contacts and there are various intermediate lithologic facies between the two rocks.

Most zircons have elongated igneous characteristics with sharp edges (up to 250 μm

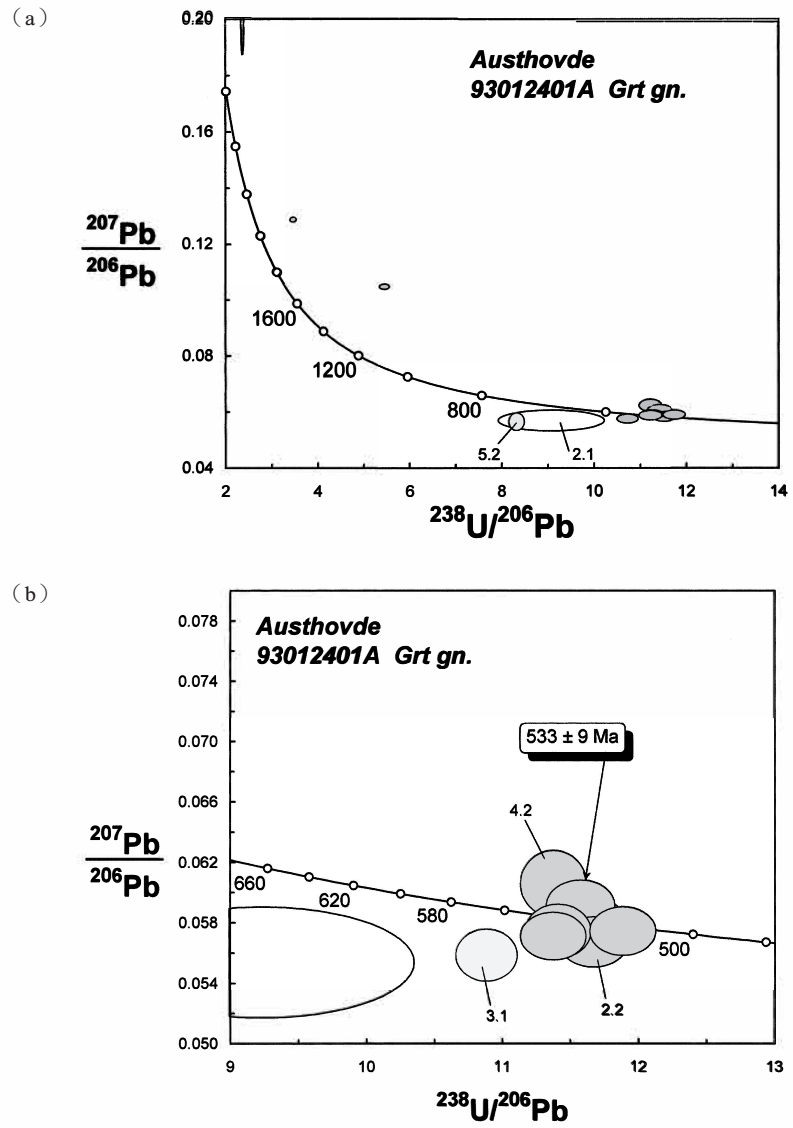

Fig. 9. Tera and Wasserburg (1972) concordia plot of uncorrected U-Pb zircon analyses for Sp. 93012401A (Austhovde). Analyses plotted with one sigma error bars. Weighted mean of $^{206}Pb/^{238}U$ ages (^{207}Pb corrected, ±95% confidence limits) is shown for the dominant grouping of near, to concordant analyses.

long) (Fig. 10a). Sixteen areas on thirteen zircons were analyzed (Fig. 11a). The analyses of thirteen grains indicate a weighted mean $^{206}Pb/^{238}U$ age of 532±8 Ma. Most of these are on oscillatory zoned spots, indicating the intrusive age of this body. Cores of three grains (9-2, 14-1, 15-1) with high U (>1400 ppm) and structureless CL images yield older $^{206}Pb/^{238}U$ ages of ~580–630 Ma. This age is in good agreement with the secondary rims (605–630 Ma) from the granulite-facies gneiss (Y80A530) nearby

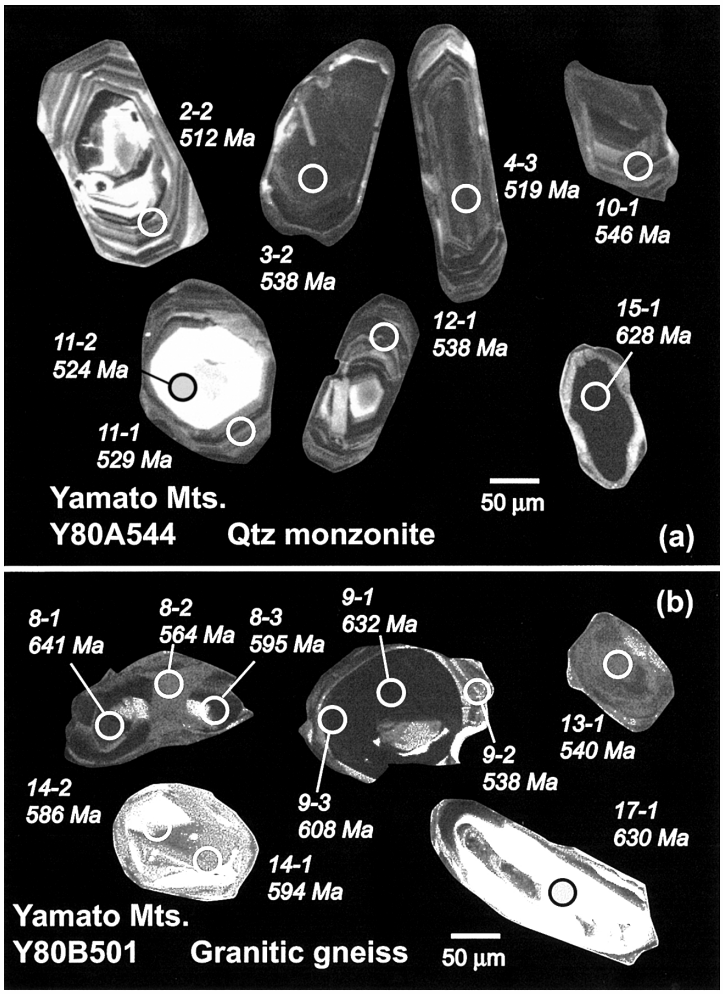

Fig. 10. Cathodoluminescence images of zircons analyzed with ion-microprobe. Spot locations and numbering and SHRIMP ages ($^{206}Pb/^{238}U$ ages) are indicated. a: Sp. Y80A544 (Massif A, Yamato Mountains), b: Sp. Y80B501 (Massif B, Yamato Mountains).

this locality. It is suggested that the older cores of the sample are derived from the country rock and survived during the magmatism.

4.5. Sample Y80B501: Granitic gneiss, Massif-B of the Yamato Mountains

This is a pink-colored granitic orthogneiss from Akakabe Bluff of Massif-B. The gneiss is the dominant rock type in the Yamato Mountains showing various migmatitic structures. The constituent minerals are biotite, plagioclase, quartz and K-feldspar with minor hornblende, allanite, zircon and magnetite. Most zircons are elongate grains with rounded ends and subrounded shapes (up to 150 μm long) (Fig. 10b). Thirty-one areas on 21 zircons were analyzed (Fig. 11b). The analyses of grain edges cluster about a weighted mean $^{206}Pb/^{238}U$ age of 539 ± 4 Ma. The core of grain 8 is

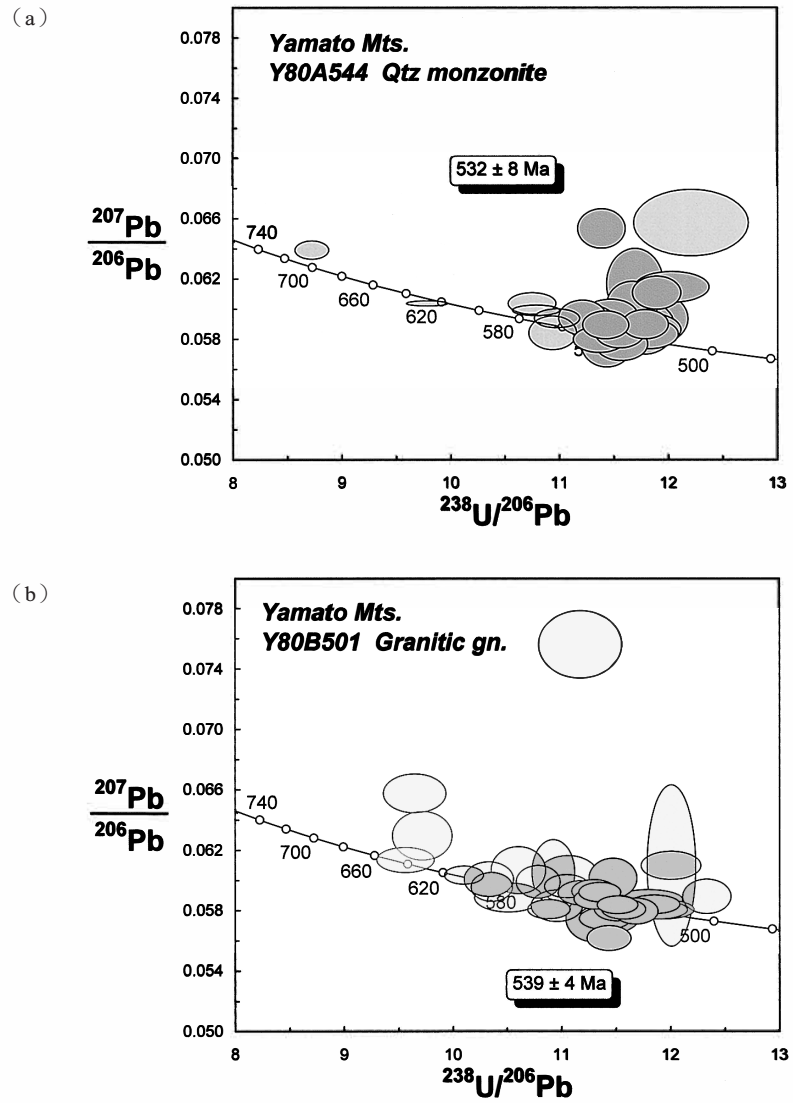

Fig. 11. Tera and Wasserburg (1972) concordia plot of uncorrected U-Pb zircon analyses for samples from the Yamato Mountains. a: Y80A544 and b: Y80B501. Analyses plotted with one sigma error bars. Weighted mean of $^{206}Pb/^{238}U$ ages (^{207}Pb corrected, ±95% confidence limits) is shown for the dominant grouping of near, to concordant analyses.

separated into two parts by the younger resorption/recrystallization. Some core analyses tending to cluster around 620 Ma (570–630 Ma) do not define a unique age because of the small number of analyses. It is also possible that they show Pb-loss at ~540 Ma. The older age is considered to indicate the timing of the emplacement of magmatic protolith and that the metamorphism took place at ~540 Ma.

5. Discussion

5.1. Pan-African event in Lützow-Holm Complex

Figure 12 shows a relative probability histogram with a range of SHRIMP U-Pb ages. Analyses shown to be derived from mixed domains by the CL studies were omitted from the plots.

It is evident that the main metamorphic event in the LHC was therefore ~520–550 Ma during the Pan-African orogeny. Fraser (1997) reported three episodes of zircon growth over ~2500 Ma detrital cores during the Pan-African from a pelitic gneiss (Sp. R-125) in Rundvågshetta; 624, 557 and 543 Ma ($^{206}Pb/^{238}U$ ages), respectively. However, the data show significant matter on the Concordia, an aspect which was acknowledged by Fraser (1997). Moreover, another pelitic gneiss (RH-112-20B) from Rundvågshetta has no indication of ~620 Ma overgrowths. Thus it is probable that the ~620 Ma overgrowth has resulted from Pb-loss from the core and that the Pan-African metamorphic event in the LHC occurred only during 550–520 Ma.

On the other hand, Nishi *et al.* (2002) reported a Sm-Nd whole-rock isochron age of 674±22 Ma with a Rb-Sr whole-rock isochron age of 583±56 Ma from Oku-iwa Rock of the Prince Olav Coast and suggested magmatism at ~680 Ma as a possibility. The ~680–780 Ma Rb-Sr whole-rock isochron ages are also reported by Shibata *et al.* (1986). However our work showed that there is no indication of ~680 Ma zircon growth in LHC. A SHRIMP U-Pb age from the same rock is required to elucidate the thermal event at the time.

5.2. Pre-Pan-African history of the Lützow-Holm Complex

The pre-history of the Pan-African event has been controversial. Many workers have suggested that Dronning Maud Land (DML) contains reworked Grenvillian basement (*e.g.* Yoshida, 1995; Jacobs *et al.,* 1998; Paech, 2001; Jacobs, 2002). On the other hand, Ikeda *et al.* (1997) reported that the ~1000 Ma Cape Hinode trondjemite in the Prince Olav Coast originated by partial melting of subducted oceanic crust, suggesting a lack of Pre-Grenvillian basement in a part of LHC. Besides Cape Hinode, there are two outcrops in LHC having ~1000 Ma U-Pb zircon ages, a garnet-biotite gneiss from Telen (Sp. 20112A) and a hornblende-biotite gneiss from Innhovde (Sp. 84011106). Fraser (1997) analyzed seven rocks from three different localities in LHC and only one granitic gneiss from Skarvsnes showed the ~1100 Ma core age of zircon. It was interpreted as the time of the intrusion of the granite.

These ~1000–1100 Ma spots were obtained only from inherited zircon cores that are considered to be magmatic. No ~1000 Ma metamorphic overgrowth of inherited zircon has been observed so far in LHC. Thus we may safely say that the ~1000 Ma event in LHC involved localized igneous activity. We assume that this activity would be related to arc magmatism although the types of magma are not known except for that of Cape Hinode. Moreover, the detrital nature of the inherited core indicates that deposition of the sedimentary protolith of the LHC occurred after the Grenvillian event as stated by Shiraishi *et al.* (1994) and Fraser (1997).

On the other hand, in Rundvågshetta, which is located at the highest metamorphic grade area in the LHC, there are no inherited Grenvillian ages but only abundant

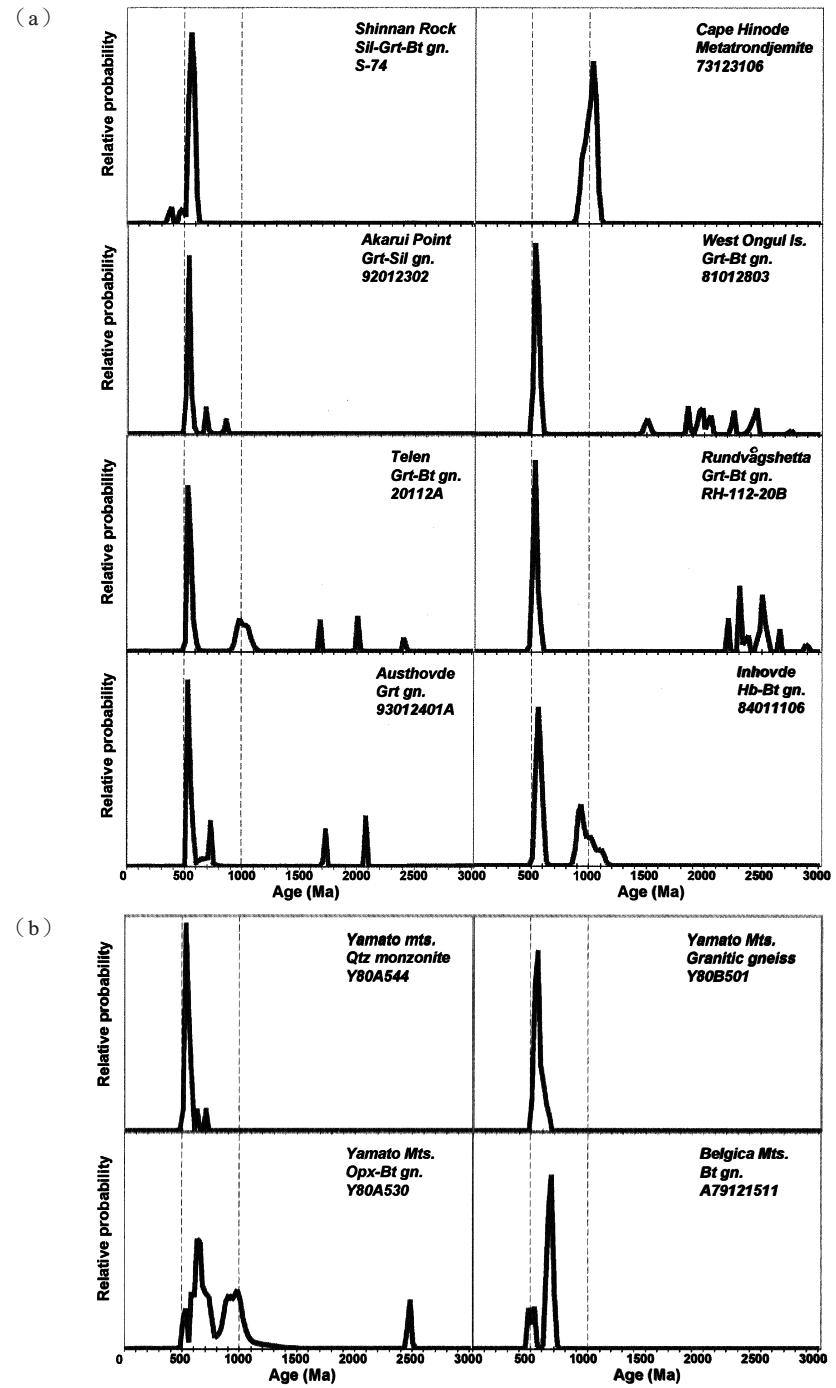

Fig. 12. Relative probability histograms showing the range of SHRIMP U-Pb ages reported by Shiraishi et al. (1994). The evident mixed ages were omitted. The $^{206}Pb/^{207}Pb$ ages were used for ages older than ~1500 Ma, while the younger ones are $^{206}Pb/^{238}U$ ages. (a) Lützow-Holm Complex, (b) Yamato-Belgica Complex.

Proterozoic and Archean cores in the pelitic gneisses as well as the West Ongul Island sample (Shiraishi *et al.,* 1994; Fraser, 1997). Such a long history of the protolith in Rundvågshetta is consistent with the results of the preliminary study on Rb-Sr whole rock analyses by Nakajima *et al.* (1987). However, it is not easy to prove the lack of Grenvillian events only from the zircon age populations. There are three possiblities. The first one is that the event did not happen. Second, it is possible that the younger thermal event effectively removed or resorbed the Grenvillian growth zones in individual zircon grains from the outcrop. Third, the number of analyses might be not enough to distingusih the Grenvillian event.

In summary we propose that the protolith of the pelitic gneisses is detritus at the margin of a pre-Grenvillian craton and that the ~1000 Ma orthogneisses are derived from the possible Grenvillian arc magmatism and do not preserve pre-Grenvillian components. This implies that the protolith of LHC is not uniform but consists of continental components of various ages and origins. This is also supported by the Nd model ages from various rocks from the LHC, which range from Archean to Neoproterozoic in age (Yoshida *et al*., 1995; Shiraishi *et al*., 1995; Shiraishi, unpublished data). In other words, LHC is a collage of small pre-Grenvillian continental blocks and Grenvillian juvenile crust (island/oceanic arcs) amalgamated by the Pan-African convergence.

To the east of the LHC, the coastal region of the Rayner Complex also lacks Grenvillian zircon growth but ~780–800 Ma zircon ages were reported (Shiraishi *et al.,* 1997). On the other hand, Grenvillian zircon core ages were reported from the inland area of the Rayner Complex (Shiraishi *et al.,* 1997). The Rayner Complex has been considered to be continuous from Kemp Land in the east, to the vicinity of Molodezhnaya Station (*e.g.* Black *et al.,* 1987). However the latter area may be a part of LHC that has not been affected by the Grenvillian event. Further study is required to elucidate the gap of metamorphic grade between amphibolite-facies Sinnan Rock and the granulite facies Molodezhnaya area.

5.3. Yamato-Belgica Complex

The two new SHRIMP U-Pb zircon ages (~535 Ma) from the Yamato Mountains are almost identical within error; if anything the quartz monzonite appears to be slightly younger than the amphibolite metamorphism. They are also similar to the peak metamorphic age in the LHC (520–550 Ma), while the early Pan-African history is not common to the two complexes (Figs. 12a and b). Although it is not well defined, the newly obtained ~570–630 Ma zircon core of the amphibolite-facies granitic gneiss (Y80501B) in the Yamato Mountains indicates the age of granite activity. The quartz monzonite also has ~630 Ma zircon cores, which might be derived from the country rocks and have survived in the monzonite magma. On the other hand, the ~605–630 Ma growth is significant in rims of the granulite-facies orthopyroxene-biotite gneiss from Massif A (Y80A530), although the SHRIMP analyses did not define a unique age or age groupings.

In summary we consider that there are two thermal events in the Pan-African age in YBC: The older event (~620 Ma in average) may be the granulite facies metamorphism associated with granite. The younger event (~535 Ma) is amphibolite facies

metamorphism with local migmatization and the quartz monzonite magmatism which followed the widespread syenitic plutonism (Shiraishi *et al.*, 1982). In the Belgica Mountains, there is a younger overgrowth surrounding the ~660 Ma overgrowth that is too narrow to analyze by SHRIMP.

The above geological setting is similar to that of the Sør Rondane Mountains, especially in the eastern part where the migmatization at ~555 Ma followed the amphibolite-facies metamorphism at ~610 Ma (Shiraishi, unpublished data).

We have not enough data to describe the pre-Pan-African history of the Yamato-Belgica Complex (YBC). However, it is possible that the oldest component was provided from the unknown craton, possibly in East Antarctica. The core and overgrowth of zircons from a pelitic gneiss (Y80A530) showing ~1000 Ma ages suggest that the Grenvillian thermal event was significant in the Yamato Mountains, although no similar age component from the Belgica Mountains has been obtained so far.

To the west of YBC in central Dronning Maud Land, Paech (2001) described Grenvillian basement rocks intruded by charnockitic granitoids and anorthosites during two Pan-African igneous episodes. This is comparable to the history of the Sør Rondane Mountains. Further discussion of the tectonic evolution of Dronning Maud Land will be reported elsewhere together with the SHRIMP data from the Sør Rondane Mountains.

6. Conclusions

1) CL images from the samples used by Shiraishi *et al.* (1994) confirm that the main metamorphic event in the LHC was the ubiquitous age of ~520–550 Ma during the Pan-African orogeny.
2) ~1000 Ma zircon growth is not recognized in the pelitic gneisses throughout the LHC, but only magmatic zircon core is recorded in the orthogneisses and a pelitic gneiss.
3) The protoliths of pelitic gneisses in the LHC were detritus at the margin of a pre-Grenvillian craton and the ~1000 Ma orthogneisses are derived from the Grenvillian juvenile crust.
4) Thus LHC is a collage of pre-Grenvillian continental blocks and Grenvillian juvenile crust amalgamated by the Pan-African convergence.
5) In contrast, YBC yields two stages of the Pan-African age; ~620 and ~535 Ma, that show a similar history to that of the Sør Rondane Mountains in the west.

Acknowledgments

We thank Drs. R. Armstrong (RSES, ANU), A. Yamaguchi (NIPR) and H. Kaiden (NIPR) for support of SHRIMP analyses. We also thank Prof. M. Asami (Okayama University) and Dr. G. Grantham (Council for Geosciences, South Africa) for their valuable comments for the draft. We acknowledge Prof. H. Kagami (Niigata University) and an anonymous reviewer for their critical reviews of the manuscript. This research was financially supported by a Grant-in-Aid for Scientific Research from the Japan Society for the Promotion of Science No.13440151 to K.S.

References

Asami, M., Suzuki, K. and Adachi, M. (1997): Th, U and Pb analytical data and CHIME dating of monazites from metamorphic rocks of the Rayner, Lützow-Holm, Yamato-Belgica and Sør Rondane Complexes, East Antarctica. Proc. NIPR Symp. Antarct. Geosci., **10**, 130–152.

Black, L.P., Harley, S.L., Sun, S.S. and McCulloch, M.T. (1987): The Rayner Complex of East Antarctica: complex isotopic systematics within a Proterozoic mobile belt. J. Metamorph. Geol., **5**, 1–26.

Boger, S.D., Wilson, C.J.L and Fanning, C.M. (2001): Early Paleozoic tectonism within the East Antarctic craton: The final suture between east and west Gondwana? Geology, **29**, 463–466.

Compston, W. (1999): Geological age by instrumental analysis. Mineral. Mag., **63**, 297–311.

Compston, W., Williams, I.S., Kirshvink, J.L., Zhang, Z. and Ma, G. (1992): Zircon U-Pb ages for the Early Cambrian time scale. J. Geol. Soc. London, **149**, 171–184.

Fitzsimons, I.C.W. (2000): A review of tectonic events in the East Antarctic shield and their implications for Gondwana and earlier supercontinents. J. Afr. Earth Sci., **31**, 3–23.

Fraser, G. (1997): Geochronological constraints on the metamorphic evolution and exhumation of the Lützow-Holm Complex, East Antarctica. Ph. D. Thesis, The Australian National University, 254 p.

Hiroi, Y., Shiraishi, K. and Motoyoshi, Y. (1991): Late Proterozoic paired metamorphic complexes in East Antarctica, with special reference to the tectonic significance of ultramafic rocks. Geological Evolution of Antarctica, ed. by M.R.A. Thomson *et al.* Cambridge, Cambridge Univ. Press, 83–87.

Ikeda, Y., Shiraishi, K. and Yanai, K. (1997): Petrogenesis of the meta-trondhjemites from Cape Hinode, East Antactica. Proc. NIPR Symp. Antarct. Geosci., **10**, 102–110.

Jacobs, J. (2002): The Mozambique Belt from an East Antarctic perspective. R. Soc. N. Z. Bull, **35**, 3–18.

Jacobs, J., Fanning, C. M., Henjes-Kunst, F., Olesch, M. and Paech, H.-J. (1998): Continuation of the Mozambique Belt into East Antarctica: Grenville-age metamorphism and polyphase Pan-African high-grade events in central Dronning Maud Land. J. Geol., **106**, 385–406.

Ludwig, K.R. (2001a): Squid 1.00: a users manual. Berkley Geochronology Center Spec. Publ., No. 2, 17 p.

Ludwig, K.R. (2001b): Isoplot/Ex rev. 2.49: a geochronological tool kit for Microsoft Excel. Berkley Geochronology Center Spec. Publ., No. 1a, 55 p.

Motoyoshi, Y. and Ishikawa, M. (1997): Metamorphic and structural evolution of granulites from Rundvågshetta, Lützow-Holm Bay, East Antarctica. The Antarctic Region: Geological Evolution and Processes, ed. by C.A. Ricci. Siena, Terra Antartica, 65–72.

Nakajima, T., Shibata, K., Shiraishi, K., Motoyoshi, Y. and Hiroi, Y. (1987): Rb-Sr whole-rock age of the metamorphic rocks from eastern Queen Maud Land, East Antarctica. The 8th Symposium on Antarctic Geosciences, Abstract and Program. Tokyo, Natl Inst. Polar Res., 15 (in Japanese).

Nishi, N., Kawano, Y. and Kagami, H. (2002): Rb-Sr and Sm-Nd isotopic geochronology of the granitoid and hornblende biotite gneiss from Oku-iwa Rock in the Lützow-Holm Complex, East Antarctica. Polar Geosci., **15**, 46–65.

Paces, J.B. and Miller, J.D.J. (1993): Precise U-Pb ages of Duluth Complex and related mafic intrusions, northeastern Minnesota: geochronological insights to physical, petrogenetic, paleomagnetic, and tectonomagmatic processes associated with the 1.1 Ga midcontinent rift system. J. Geophys. Res., **98**, 13997–14013.

Paech, H-J. (2001): Pervasive pan-African reactivation of the Grenvillian crust and large igneous intrusions in central Dronning Maud Land, East Antarctica. Continental Reactivation and Reworking, ed. by J.A. Miller *et al.* London, Geological Society, 343–355 (Geol. Soc., London, Spec. Pub., 184).

Rubatto, D. and Gebauer, D. (2000): Use of cathodoluminescence for U-Pb zircon dating by ion microprobe: some examples from the Western Alps. Cathodoluminescence in Geosciences, ed. by M. Pagel *et al.* Berlin, Springer, 373–414.

Shibata, K., Yanai, K. and Shiraishi, K. (1986): Rb-Sr whole-rock ages of metamorphic rocks from eastern Queen Maud Land, East Antarctica. Mem. Natl Inst. Polar Res., Spec. Issue, **43**, 133–148.

Shiraishi, K., Asami, M. and Ohta, Y. (1982): Plutonic and metamorphic rocks of Massif-A in the Yamato Mountains, East Antarctica. Mem. Natl Inst. Polar Res., Spec. Issue, **21**, 21–31.

Shiraishi, K., Hiroi, Y., Ellis, D.J., Fanning, C.M., Motoyoshi, Y. and Nakai, Y. (1991): The first report of a Cambrian orogenic belt in East Antarctica - an ion microprobe study of the Lützow-Holm

Complex. Recent Progress in Antarctic Earth Science, ed. by Y. Yoshida *et al.* Tokyo, Terra Sci. Publ., 67–73.

Shiraishi, K., Ellis, D.J., Hiroi, Y., Fanning, C.M., Motoyoshi, Y. and Nakai, Y. (1994): Cambrian orogenic belt in East Antarctica and Sri Lanka: implications for Gondwana assembly. J. Geol., **102**, 47–65.

Shiraishi, K., Kagami, H. and Yanai, K. (1995): Sm-Nd and Rb-Sr isochron ages for meta-trondhjemites from Cape Hinode, East Antarctica. Proc. NIPR Symp. Antarct. Geosci., **8**, 130–136.

Shiraishi, K., Ellis, D.J., Fanning, C.M., Hiroi, Y., Kagami, H. and Motoyoshi, Y. (1997): Re-examination of the metamorphic and protolith ages of the Rayner complex, Antarctica: Evidence for the Cambrian (Pan-African) regional metamorphic event. The Antarctic Region: Geological Evolution and Processes, ed. by C.A. Ricci. Siena, Terra Antartica, 79–88.

Tera, F. and Wasserburg, G.J. (1972): U-Th-Pb systematics in three Apollo 14 basalts and the problem of initial Pb in Lunar rocks. Earth Planet. Sci. Lett., **14**, 281–304.

Vavra, G., Gebauer, D., Schmid, R. and Compston, W. (1996): Multiple zircon growth and recrystallization during polyphase Late Carboniferous to Triassic metamorphism in granulites of the Ivrea Zone (Southern Alps): an ion microprobe (SHRIMP) study. Contrib. Mineral. Petrol., **122**, 337–358.

Vavra, G., Schmid, R. and Gebauer, D. (1999): Internal morphology, habit and U-Th-Pb microanalysis of amphibolite-to-granulite facies zircons: geochronology of the Ivrea Zone (Southern Alps). Contrib. Mineral. Petrol., **134**, 380–404.

Williams, I.S. (1998): U-Th-Pb geochronology by ion microprobe. Rev. Econ. Geol., **7**, 1–35.

Yoshida, M. (1995): Assembly of East Gondwana during the Mesoproterozoic and its rejuvenation during the Pan-African period. Geol. Soc. India, Mem., **34**, 22–45.

Yoshida, M., Kagami, H. and Unnikrishnan-Warrier, C. (1995): Preliminary measurement of Neodymium model ages for rocks from Lützow-Holm Bay area, East Antarctica. The 15th Symposium on Antarctic Geosciences, Program and Abstracts. Tokyo, Natl Inst. Polar Res., 44.